Published in final edited form as:
Biochim Biophys Acta. 2009 June ; 1788(6): 1229–1237. doi:10.1016/j.bbamem.2009.03.017.

Macroscopic domain formation during cooling in the platelet plasma membrane: an issue of low cholesterol content

Rachna Bali[a], **Laura Savino**[b], **Diego A. Ramirez**[b], **Nelly M. Tsvetkova**[c], **Luis Bagatolli**[d], **Fern Tablin**[e], **John H. Crowe**[a], and **Chad Leidy**[a,b]

a *Department of Molecular and Cellular Biology, University of California, Davis, CA, USA*

b *Department of Physics, Universidad de los Andes, Bogotá, Colombia*

c *Bayer-Healthcare, Berkeley, CA, USA*

d *MEMPHYS Center for Biomembrane Physics, Department of Biochemistry and Molecular Biology, University of Southern Denmark, Odense, Denmark*

e *School of Veterinary Medicine, Anatomy, Physiology and Cell Biology, University of California, Davis, CA, USA*

Abstract

There has been ample debate on whether cell membranes can present macroscopic lipid domains as predicted by three-component phase diagrams obtained by fluorescence microscopy. Several groups have argued that membrane proteins and interactions with the cytoskeleton inhibit the formation of large domains. In contrast, some polarizable cells do show large regions with qualitative differences in lipid fluidity. It is important to ask more precisely, based on the current phase diagrams, under what conditions would large domains be expected to form in cells. In this work we study the thermotropic phase behavior of the platelet plasma membrane by FTIR, and compare it to a POPC/Sphingomyelin/Cholesterol model representing the outer leaflet composition. We find that this model closely reflects the platelet phase behavior. Previous work has shown that the platelet plasma membrane presents inhomogeneous distribution of DiI18:0 at 24°C, but not at 37°C, which suggests the formation of macroscopic lipid domains at low temperatures. We show by fluorescence microscopy, and by comparison with published phase diagrams, that the outer leaflet model system enters the macroscopic domain region only at the lower temperature. In addition, the low cholesterol content in platelets (~15 mol %), appears to be crucial for the formation of large domains during cooling.

Keywords

lipid membrane thermodynamics; platelets; lipid domain formation; liquid-ordered phase; cholesterol; FTIR; lipid rafts; lipid platforms

Corresponding author: Chad Leidy, e-mail: E-mail: cleidy@uniandes.edu.co, fax: (+571) 339-4949 ext. 2712, Department of Physics, Universidad de los Andes, Carrera 1 N° 18A 10, Bogotá, Colombia.

1. Introduction

Ever since the first images of macroscopic lipid domains in giant unilamellar vesicles involving liquid-ordered/liquid-disordered phase separation [1], there has been great interest in detecting these large-size lipid domains in vivo. However, this effort has not yielded many clear examples in cell membranes, which has even lead to doubts regarding the possibility of domain formation in cells [2,3]. Through spectroscopy techniques, however, lipid domains have been confirmed to be present in cells [4]. But, although macroscopic lipid domains appear in the visible size range in artificial membranes [5–7], in live cells, lipid domains normally range in the tens of nanometers, and appear to be transient [8–10]. Several groups argue that the formation of macroscopic lipid domains is hindered in live cell membranes by interactions with intermembrane proteins [11] and the cytoskeleton [9]. When cytoskeleton-free giant plasma membrane vesicles (GPMVs) are formed from cells, macroscopic domains appear on the surface of the GPMVs, indicating that the cytoskeleton restricts the growth of domains [12].

Macroscopic membrane regions with distinct physical properties are not completely absent in cell systems. The membrane surface of polarizable cells can present clearly defined regions at a macroscopic scale. For example, two-photon microscopy using 6-acyl-2-dimethylaminonaphthalene (laurdan) as a reporter probe has shown macroscopic regions with marked differences in membrane packing in macrophages [13]. T lymphocytes also require large regions of the membrane to become differentiated during cell migration, and the segregation of lipid phases appears to aid in this differentiation by partitioning the membrane protein agents needed for chemotaxis into the leading edge and the uropod of the cell [14]. T-cells also form large specialized membrane regions during synaptic immune formation, and this has also been shown to involve the formation of regions enriched in cholesterol and sphingomyelin, which is indication of the possible formation of a liquid-ordered phase [15, 16]. However, it is not clear whether these examples are driven through lipid phase separation.

In a recent meeting focusing on lipid rafts [17], a consensus was reached regarding the definition of cholesterol-enriched domains (rafts) and the origin of these larger platforms. It was agreed that “Membrane rafts are small (10–200 nm), heterogeneous, highly dynamic, sterol- and sphingolipid-enriched domains that compartmentalize cellular processes. Small rafts can sometimes be stabilized to form larger platforms through protein-protein and protein-lipid interactions.” Therefore, for platform formation only protein-protein and protein-lipid interactions were considered as driving forces. There was not enough evidence to consider lipid phase separation as a driving force for macroscopic platform formation in cells in this working definition. This was supported by the fact that, with a few exceptions [13,18,19], large lipid domains have not been detected in steady state cells. In addition, in the cases where platform formation is observed this appears to be induced by stimulation, which is not lipid driven. It is clear, for example, that in the immunological synapse, the dynamic formation of large platforms appears to be protein mediated [16,20].

The absence of evidence for lipid-induced platform formation in cell membranes does not necessarily imply that large scale lipid phase separation is always inhibited by membrane proteins. It is important to consider that the temperature and composition conditions may not be adequate for generating large scale lipid phase separation in cells. We suggest that the underlying reason for the discrepancy between the model studies and cells studies lies in the use of an inappropriate model system for comparison. Early experiments used the DOPC/SM/Cholesterol ternary mixture as a model to mimic the membrane outer leaflet composition [1]. This mixture presented a conveniently large compositional regime showing macroscopic domains in giant unilamellar vesicles. The two unsaturated chains in DOPC ensure a marked phase separation from SM and a strong steric hindrance in the interaction with cholesterol, which generates a broad compositional regime of liquid-ordered/liquid-disordered phase

separation [7,21]. However, in the plasma membrane of cells the prevalent low melting temperature unsaturated lipid is POPC and not DOPC. POPC has only one unsaturated chain, and for this reason, the POPC/SM/Cholesterol phase diagram presents a much narrower region of macroscopic phase separation, as evidenced from fluorescence microscopy on giant unilamellar vesicles [21]. Careful examination of the POPC/SM/Cholesterol phase diagram indicates that only those membranes that present low cholesterol contents (below 20 mol %) will access the compositional region of macroscopic domains [21]. It is therefore important to investigate, based on the POPC/SM/Cholesterol phase diagram, what cell systems may present the appropriate composition to provide a driving force for macroscopic lipid phase separation

In this context, the platelet plasma membrane presents an interesting thermally sensitive system. Human platelets are very susceptible to chilling, activating when the temperature falls below 20°C [22,23]. This limitation represents a crucial issue in terms of storage of platelets in blood banks. Platelets need to be stored above 20°C to avoid activation, and therefore are prone to bacterial contamination [24]. Recent work attempting to explain cold-induced activation in platelets has shown that DiI-C18:0 becomes inhomogeneously distributed in the platelet plasma membrane below 24°C [25]. This uneven distribution of DiI-C18:0 suggests the generation of macroscopic lipid phase separation during cooling. However, above 24°C, an even distribution of the dye is observed. This reversibility suggests that domain formation is thermotropically driven, since biochemical signaling would be expected to induce non reversible aggregation. With regards to the composition of the platelet plasma membrane, human platelets contain a low cholesterol content around 15 mol% [26], which places them close to the compositional regime of macroscopic domain formation reported for POPC/SM/Cholesterol [21]. For this reason, the platelet presents an interesting opportunity to compare with the model system phase diagrams.

In order to generate an appropriate model system, we select a POPC/SM/Cholesterol ternary mixture chosen to reflect the reported composition of the platelet plasma membrane. We compare the thermotropic phase behavior of the model system and the platelets by FTIR. This is done by following the lipid CH_2 stretch band by Fourier transform infrared spectroscopy (FTIR). This band reports the level of lipid chain order, and has been used extensively to measure solid-ordered to liquid-disordered phase transitions (T_m) in model membranes [27, 28]. We then explore macroscopic domain formation in giant unilamellar vesicles by fluorescence microscopy in the model system to determine the conditions where macroscopic domains are expected.

Several POPC/SM/Cholesterol phase diagrams reporting regions of liquid-ordered (*lo*)/liquid-disordered (*ld*)/solid-ordered (*so*) phase coexistence have been published in recent years [21, 29,30]. It appears that the reported regions of phase coexistence for this particular system vary qualitatively depending on the technique used to detect them. Broad regions of *lo*/*ld* phase coexistence are reported when using spectroscopic techniques that detect nanoscopic or mesoscopic domains [29,30]. Narrower regions of *lo*/*ld* phase coexistence are reported when detecting larger domains by fluorescence microscopy [21]. It would be expected that macroscopic phase separation in platelets during cooling should reflect the phase diagrams determined by fluorescence microscopy, and therefore we choose to focus on the phase diagrams that detect macroscopic domains in order to determine whether the platelet plasma membrane could generate large phase separated regions.

2. Materials and Methods

2.1. Reagents

1-Palmitoyl 2-oleoyl-phosphatidylcholine (POPC), deuterated 1-palmitoyl 2-oleoyl-phosphatidylcholine (POPC-d31), porcine brain sphingomyelin (BSM), and cholesterol were

purchased from Avanti Polar Lipids (Alabaster, AL) and where used without further purification. 1,1′-dioctadecyl-3,3,3′,3′-tetramethylindocarbocyanine perchlorate (DiI_{C18}) was purchased from Molecular Probes (Invitrogen, Copenhagen, Denmark). Sphingomyelinase (SMase) from Bacillus cereus and methyl-β-cyclodextrin (MβCD) were purchased from Sigma (Saint Louis, MO).

2.2. Sample Preparation

2.2.1. Platelet isolation—Platelets were obtained from the Sacramento Blood Center or from human volunteers, with informed consent, according to institutional protocols. Platelets were pelleted and washed three times (320g for 14 min, 480 g for 22 min and 480 g for 15 min) in Buffer A (100 mM NaCl, 10 mM KCl, 10 mM EGTA, 10 mM imidizole, pH 6.8) containing 10 mg/ml prostaglandin E [31].

2.2.2. Preparation of large unilamellar vesicles (LUVs)—Appropriate amounts of POPC and SM were dissolved and mixed in chloroform. The samples were then dried under nitrogen gas and placed under vacuum overnight to remove the residual solvent. The dry lipids were dispersed in Buffer A to a final concentration of 50 mM. For SMase treated LUVs, 3 mM $MgCl_2$ was added to the buffer before LUV preparation. Aqueous multilamellar lipid dispersions were prepared by heating the sample to 65°C, followed by vortexing. This procedure was repeated multiple times for a total of 20 min. Large unilamellar vesicles were prepared by extruding the suspension 15 times through a hand-held Lipofast extruder (Avestin, Ottawa, Canada) with two stacked 0.1-mm pore size polycarbonate filters (Poretics, Livermore, CA).

2.2.3. MβCD and SMase treatment—Washed platelets were concentrated to a final concentration of 1×10^8 cells/ml. For cholesterol depletion, washed platelets were incubated for 1 h at 37°C and then were treated with MβCD (10 mM) in Buffer A for 1 h at 37°C. For SMase treatment 1 ml of MβCD treated platelets or LUVs were incubated in Buffer A with 3 mM $MgCl_2$ in the presence of 5 units of SMase for 30 min or 1 h at 37°C. No significant differences were observed when comparing the samples treated for 30 min and 1 hr, indicating that the reaction had reached completion.

2.2.4. Giant unilamellar vesicle (GUV) preparation—GUVs were obtained by the electroformation method first described by Angelova et al. [32] on a home built Teflon chamber using Pt electrodes to avoid oxidation. 3 μl of a 0.2 mg/ml lipid/chloroform mixture labeled with 0.4 mol% 1,1′-dioctadecyl-3,3,3′,3′-tetramethylindocarbocyanine perchlorate (DiI_{C18}) was deposited on each Pt electrode. The sample was then placed overnight under vacuum to remove traces of the organic solvent. Sufficient amounts of 200 mOsM sucrose solution (17.5 MΩ; Millipore, Billerica, MA) were then added to the Pt electrodes to cover them completely, and a low frequency AC field was applied using a function generator (Vann Draper Digimess Fg 100, Stenson, Derby, UK; sine function, freq. 10 Hz, amplitude 2 V) for 1–2 h. The temperature used for GUV formation was well above the fluid/gel phase transition temperature (~80°C for all samples). After vesicle formation, the AC field was turned off and the vesicles were transferred to an iso-osmolar glucose solution in a special chamber (200 μl of glucose + 50 μl of the GUVs in sucrose in each of the eight wells of the plastic chamber used; LabTek, Naperville, IL). This induces the GUVs to settle on the chamber bottom surface, allowing more stable visualization.

2.3. FTIR of platelets and unilamellar vesicles

For the platelet FTIR measurements, treated and untreated platelets where were pelleted for 1 minute at 1200g and a 5-μl volume of the pellet was placed between two FTIR CaF windows. For the LUV FTIR 2 measurements, a 5-μl volume of LUVs at the same concentration as

indicated in sample preparation was placed on the FTIR windows. IR spectra were recorded on a Perkin-Elmer 2000 Fourier transform IR-spectrometer (Perkin-Elmer, Norwalk, CT) equipped with a liquid-nitrogen-cooled mercury/cadmium/telluride (MCT) detector interfaced to a computer with Spectrum 2000 software. Temperature was controlled by a Peltier device and monitored by a thermocouple placed on the FTIR window. Infrared spectra in the CH stretching region from 3000 to 2800 cm^{-1}, and CH_2 stretching region CD_2 from 2200 to 2000 cm^{-1} were monitored as a function of temperature. Eight spectra were averaged at each temperature point. Spectra were continuously acquired at a temperature increase rate of 3°C/min. Phase transitions were determined by plotting the band positions of the CH_2 symmetric and CD_2 asymmetric stretch modes. The band positions were determined by taking the inverted second derivative of the original spectra and averaging the band intercepts at 80% intensity. The symmetric CD_2 stretch mode is less intense than the asymmetric mode, and it appears as a poorly defined shoulder for the lipid concentrations studied. Therefore, to obtain a less noisy phase transition measurement we followed the more intense asymmetric CD_2 stretching vibration for the deuterated species. Conversely, we used the symmetric CH_2 stretch mode to monitor phase transitions for nondeuterated species, because this mode is more widely used for nondeuterated lipids. There appears to be no appreciable difference between measurements of the phase transition using the symmetric and asymmetric CH_2 stretch modes. First derivatives of thermograms were calculated by a 13 point Savitzky-Golay smoothing procedure of the raw data through Table Curve from Systat Software, Inc. (San Jose, CA). First derivatives are only used as a visual aid to accent the inflection points in the raw thermograms.

2.4. Fluorescence microscopy of giant unilamellar vesicles

An inverted confocal fluorescence microscope (Zeiss model No. LSM 510 META NLO; Carl Zeiss, Jena, Germany) was used to visualize the giant vesicles. The excitation wavelength was 543 nm, and the fluorescence was collected using bandpass filter of 590/625 nm. The objective used for the experiments were a 40X water immersion, NA 1.2, and a 20X air objective, NA 0.75. The GUVs fluorescent images were obtained at the polar region of the GUVs, i.e., the north or south pole of the vesicle (the circumpolar region).

3. Results

3.1 Platelet thermotropic behavior as measured by FTIR

Figure 1A shows the thermotropic phase behavior of human platelets as measured by monitoring the CH_2 symmetric stretch band by FTIR. This vibration is sensitive to the level of gauche rotamers in the chains, which is an indicator of the phase state of the membrane. A phase transition from *so* to *ld* appears as a sharp upward shift in the wavenumber. Fig. 1A shows that fresh platelets containing cholesterol do not present clear cooperative events, which is explained by the broadening of the *so* to *ld* phase transition by cholesterol [25, 33, 34]. This broadening results from the fact that, due to its rigid structure and its close interactions with the chain groups, the presence of cholesterol increases the chain order in the *ld* phase [33]. By removing cholesterol from the platelets, the *ld* to *so* phase transitions become apparent [25]. In this way, we can explore in more detail the underlying thermotropic behavior of the platelet components in the absence of the attenuating effect of cholesterol. After depletion of cholesterol by β-CD (Fig. 1A, ▲), we find two cooperative events at 15°C (top left arrow) and 37°C (top right arrow). Since SM is the only major lipid component with a high phase transition temperature in healthy eukariotic cells, it is likely that the cooperative event at 37°C involves a SM rich population. In order to confirm the identity of the 37°C melting event, we treat platelets with sphingomyelinase (SMase). This treatment should result in the hydrolysis of sphingomyelin and the formation of ceramides [35], which are characterized by having much higher melting temperatures [36]. Indeed, after treatment with sphingomyelinase (SMase), a higher T_m event appears near 47°C while the 37°C event disappears (Fig. 1A, ○). This shift in

the cooperative event is clearly observed when comparing the first derivatives of the thermotropic traces before and after SMase treatment (Fig. 1B). These results, in general, corroborate that the cooperative event at 37°C is due to a SM rich population. The position of the SM cooperative melting event in platelets, which occurs at 37°C, serves as a reference temperature that can be used to compare with the POPC/SM/Cholesterol model presented in the next section. The model should present a melting event involving the SM rich population at a similar temperature compared to the SM event in platelets. The 15°C cooperative event that appears in the platelet melting profile must correspond to a lower melting temperature population, which will be modeled by POPC.

3.2. Outer leaflet model of the platelet plasma membrane

In order to build a model that reflects as closely as possible the platelet phase behavior, we consider its composition. Previous research shows, as indicated in Table 1, that the platelet plasma membrane is composed (by weight percent) of ~35% PC (phosphatidylcholine), ~25% PE (phosphatidylethanolamine), ~15%SM (sphingomyelin) ~12% of PS and PI (phosphatidylserine and phosphatidylinositol) ~7.5% cholesterol, and ~5.5% other [26]. As with other cell systems, this lipid population is asymmetrically distributed among the two bilayer leaflets within the platelet plasma membrane [35]. All the SM is found in the outer leaflet while the inner leaflet contains PE, PS, PI. PC's are found in both leaflets, but their distribution is skewed towards the outer leaflet. Due to its fast transfer rate, cholesterol is expected to partition equally in both leaflets [37]. This membrane asymmetry implies that the outer leaflet will resemble a composition of approximately 55:30:15 (molar ratio) PC/SM/Cholesterol, which takes into account that cholesterol, has approximately half the molecular weight of the other two components (Table 1).

Inner leaflet lipids are expected to be mostly unsaturated, therefore presenting melting temperatures below 0°C. In addition, studies using model systems that mimic the inner leaflet composition have shown that these lipids do not drive lipid phase separation and domain formation [38]. We therefore expect that the inner leaflet lipids do not participate strongly in the thermal events occurring above 0°C, and that the outer leaflet composition presented in the fifth column in Table 1 will model the total thermotropic cooperative events indicated by the arrows in Fig. 1. Additionally, Fig. 1B and C show that after treatment of platelets with SMase the cooperative event at 37°C disappears completely. This indicates that the high T_m melting event is a SM rich population located in the outer leaflet, since no residual inner leaflet SM remains. An additional piece of information that justifies the assumption that macroscopic domain formation observed in platelets should result from the thermotropic phase behavior of the outer leaflet model is that the large domains observed in platelets by Gousset et al. were visualized by incorporating DiI to the outer leaflet [25]. It could be argued that the inner and outer leaflets are not completely uncoupled, but for a first approximation we use a model based on the outer leaflet composition to compare with the platelet thermotropic behavior.

3.3. Thermotropic behavior of the outer leaflet model as measured by FTIR

Figure 2A shows the thermotropic phase behavior of the 55:30 POPC/SM model system in the presence and absence of 15 mol% cholesterol. In the absence of cholesterol, we also observe two cooperative events. These events appear at 10 and 27°C, which is several degrees away from the thermal events observed for platelets at 15°C (top left arrow) and 37°C. This discrepancy is not unexpected since we are not using the full composition of the platelet outer leaflet. We believe that this shift results from not taking into account higher melting PCs such as DPPC and SOPC which also represent a significant fraction of the PC population in the outer leaflet. In order to identify independently the thermal events related to the POPC population and the SM population, we use deuterated POPC (Fig. 2B). The deuterated palmitoyl chain in POPC-d31 presents a shift in its vibration frequency of approximately 800

cm^{-1}, which allows us to distinguish the POPC melting event from the SM melting event. The deuterated/undeuterated system shows clearly that the event at 10°C is related to a POPC rich population, while the event at 27°C is related to a SM rich population. The use of deuterated lipids results in a downward shift of a couple of degree in the melting temperature that should be considered when comparing the deuterated from the undeuterated mixtures [27]. In POPC-d31 only the palmitoyl chain is dueterated, which implies that a CH_2 stretch signal should also originate from the oleo chain in POPC. However, for this sample less than half of the total CH_2 vibrational groups correspond to the oleyl vibrations. From Fig. 2A it is evident that the oleoyl vibrations do not contribute strongly to the CH_2 signal since a POPC cooperative event is not distinguishable at 10°C in the CH_2 stretch thermogram (Fig. 2B, closed triangles) as expected based on the deuterated signal (Fig. 2B, open circles).

Treatment with SMase of the 55:30 POPC/SM model system also results in the appearance of a higher melting event beginning at 50°C (Fig. 2A). The emergence of a high melting temperature event is seen when comparing the first derivatives of the thermotropic traces before and after treatment (Fig. 1C). It is important to note that there is a residual melting event at 30°C remaining after SMase treatment, suggesting that not all sphingomyelin became hydrolyzed. Since the methodology for preparing these large unilamellar vesicles does not induce asymmetry we expect that SM will be equally distributed in the inner and outer leaflets of the vesicles. This residual thermal event at 30°C would correspond to the SM in the inner leaflet of the vesicles since the artificial vesicles are symmetric. This result also corroborates that the SM in the platelet is asymmetrically distributed, and that the 37°C cooperative event solely corresponds to the outer leaflet SM.

3.4. Comparison between the thermotropic phase behavior of the platelet and the outer leaflet model

Figure 3 shows a comparison between the model system and the platelet plasma membrane phase behavior. It is clear from the comparison that the cooperative event related to the sphingomyelin-rich population in the model matches well with what is observed in platelets (Fig. 3A, and 3B). The main difference between the model system and the platelets is that the total wavenumber shift between the low temperature *so* phase and the high temperature *ld* phase is wider in the model system. More specifically, the platelets show a higher wavenumber in the *so* temperature range (around 0°C) compared to the model, indicating that the platelets present a higher level of fluidity at low temperatures. At high temperatures the wavenumber for the platelets and the model match closely. This discrepancy at low temperatures very likely results from the fact that the inner leaflet components in the platelet plasma membrane are still in the fluid phase. Therefore, the overall level of fluidity in the platelet plasma membrane is higher at low temperatures compared to the model. At higher temperatures when all the components in the model and the platelet have melted the level of fluidity is the same for both systems. In general, the thermotropic phase behavior of the platelet and the model system are very similar, in particular with regards to the position of the high temperature cooperative event related to the sphingomyelin population.

When comparing the platelet thermotropic phase behavior and the model system in the presence of cholesterol (Fig. 3B), with the exception of the wavenumber divergence at low temperatures, there is still a close similarity between the two systems. It is important to notice that at high temperatures both platelets and the model system present the same degree of reduction in the wavenumber due to the formation of the *lo* phase (about 0.5 cm^{-1}). For a SM/Cholesterol system, the wavenumber above the *so*/ *ld* phase transition temperature decreases approximately linearly with cholesterol content [39]. Therefore, the wavenumber reduction is a good indicator of the amount of cholesterol in the membrane. The similarity between the platelets and the

model in this regard indicates that the 15 mol% cholesterol content in platelets reported in [26] is representative of the platelet composition.

3.5. A model system assuming no lipid asymmetry does not reflect the thermotropic lipid behavior in platelets

In order to show that the thermotropic behavior of the asymmetrically distributed outer leaflet serves as a good representation of the overall phase behavior of the platelet plasma membrane, we compare the platelet behavior with a model that assumes no asymmetry (an even distribution of lipids). That is, we analyze a mixture represented by the overall PC/SM ratio (70:15) in the platelet plasma membrane after depletion of cholesterol, instead of the PC/SM (55:30) asymmetric ratio. Although column 2 in table 1 shows that the PC/SM ratio is closer to 35:15 (wt% or mol% assuming equal molecular masses), in order to represent the symmetric plasma membrane composition a PC/SM ratio of 70:15 was used instead. The reason for this is that the 70:15 ratio accounts for the PE, PS and PI that would be present in the outer leaflet due to loss of membrane asymmetry. Although PE, PS, and PI present different physical properties than PC, these lipids would also be considered to be in the liquid-disordered phase at room temperature and in first approximation they can be represented by the PC fraction. The 70:15 ratio is the best approximation to the symmetric composition while still maintain the three-component model system we are assessing. The symmetric model uses half of the sphingomyelin content compared to the asymmetric system, since in this symmetric model the total sphingomyelin is assumed to partition evenly between the two leaflets. It is clear from Fig. 4A that the cooperative events present in the symmetric model are considerably shifted from the cooperative events in platelets. As shown in the deuterated system (Fig. 4B) the sphingomyelin melting event appears below 20°C compared to 37°C in platelets, and the POPC melting event appears at 0°C compared to 15°C in platelets. These results show that, as expected, asymmetry plays a crucial role in determining the phase behavior of the platelet plasma membrane. The model that assumes asymmetric distribution matches more closely with the phase behavior of the platelet (Fig. 3).

3.6. Macroscopic domain formation in giant vesicles reflecting the outer leaflet platelet plasma membrane composition

We investigated the formation of macroscopic domains in giant unilamellar vesicles representative of the outer leaflet composition of the platelet plasma membrane, exploring the conditions that result in macroscopic domain formation as observed in platelets. In figure 5, DiI18:0 labeled 55:30 POPC/brain sphingomyelin giant unilamellar vesicles at different cholesterol levels (0, 15, and 30 mol% cholesterol) are visualized by fluorescence microscopy. At 24°C the 0% cholesterol sample shows macroscopic *ld*/*so* domain formation for this composition. Macroscopic domains are still observed at 15 mol% cholesterol, which reflects the cholesterol content in platelets. The irregular shape of the domains in the presence of 15 mol% cholesterol suggests that the system is most likely in either the *ld*/*so* or *lo*/*ld*/*so* coexistence region. No round domains, which are representative of *lo*/*ld* coexistence, were observed as reported previously for this composition [21]. This difference may be due to the use of brain sphingomyelin instead of palmitoyl sphingomyelin. Brain sphingomyelin presents a complex mixture of sphingolipids, with some components having longer saturated chains such as 20:0, 22:0, 24:0 (Technical Specifications, Avanti Polar Lipids, Alabaster, AL). At 30 mol% cholesterol, which is double the platelet cholesterol content, no macroscopic phase separation was observed. A recent study noted that the use of a high level of light intensity during imaging induces *lo/ld* domain formation for mixtures of POPC/SM/Cholesterol giant vesicles using different SM species [40]. This study is likely to lead to a revision of phase diagrams determined through light microscopy such as the one shown in Fig. 5, at least with regards to *lo/ld* phase coexistence. In our samples we did not observe the gradual formation of *lo*/*ld* phase separation under our illumination conditions, indicated by the appearance of round

domains. Instead, we only observed irregular domains that are stable during visualization, which appears to indicate that light-induced domain formation is not occurring for our imaging conditions and dye concentrations. These investigators have not yet reported a phase diagram for POPC/SM/Cholesterol composition showing the *so*/*ld* coexistence regime [40]. Therefore, a direct comparison with their results cannot be performed at this time.

In Figure 5 we compare our observations on GUVs with a previously reported phase diagram for this system. Our results correlate well with this phase diagram at 24°C [21] where at 30 mol % cholesterol no domains are observed (top arrow, open circles Fig. 5A). Only at 15 mol % cholesterol the GUVs enter a macroscopic domain region (middle arrow, closed circles Fig. 5A) at this temperature. The authors indicate that this is a region of *lo*/*ld* coexistence. Our results indicate that macroscopic phase separation involves the *so* phase. These results clearly state that only for low cholesterol content will there be macroscopic domain formation at this temperature for this particular outer leaflet composition. It is important to note that cooling experiments with human erythrocytes that have been labeled with DiI18:0 do not show macroscopic domain formation at lower temperatures [41], which agrees with our results since the cholesterol content in erythrocyte membranes is usually above 40 mol% [42]. This would give an alternative explanation as to why many other cell systems do not show macroscopic domains, which may not appear because the cell systems are not in the appropriate compositional regime. On the other hand, nanoscopic domains are regularly detected in a variety of cells. In this regard, POPC/SM/Cholesterol phase diagrams determined through spectroscopic techniques that detect nanoscopic phase separation show much broader regions of *lo*/*ld* coexistence, which could encompass the compositions of these cells [29,30]. A broad survey of outer leaflet plasma membrane compositions for a variety of cell systems is needed to corroborate these assumptions.

Our results with giant unilamellar vesicles also agree well with the behavior in platelets at 37° C. We observe that at this temperature the 15 mol% cholesterol sample enters a one phase region and the macroscopic domains disappear (Fig. 5B). This is the same result as observed by Gousset et al. with platelets before cooling and during rewarming [25].

4. Discussion

Our results show that a POPC/SM/Cholesterol mixture reflecting the outer leaflet composition of the platelet plasma membrane mimics the lipid thermodynamic behavior of platelets as measured by FTIR. In particular, the presence of a high temperature melting event in the model, involving a SM enriched population, matches with a SM enriched population identified by SMase treatment in platelets. A significant discrepancy between the model and the platelets occurs at lower temperatures, where the CH_2 stretch vibration in the platelet sample presents a higher wavenumber than the outer leaflet model. We explain this by the fact that the outer leaflet model does not take into account the lower melting temperature species of the platelet inner leaflet. The inner leaflet lipids are expected to remain in the liquid-disordered phase around 0°C, therefore increasing the average wavenumber in the platelet sample.

Giant vesicles with a composition reflecting the outer leaflet of the platelet plasma membrane only present macroscopic segregation of DiI18:0 into distinct regions as the temperature is lowered to 23°C. No macroscopic domains are observed in the model system at 37°C. This matches with observations done in platelets [25]. In addition, in the presence of 30 mol% cholesterol no macroscopic domains are observed at either temperature, reflecting what has been previously observed in erythrocyte membranes [42]. We therefore find that the key factor that appears to lead to macroscopic domain formation in platelets is a low cholesterol content, which permits the POPC/SM/Cholesterol mixture to access a region of macrodomains as temperature is lowered. The fact that macroscopic domain formation in platelets is reversible

supports the notion that this event is not driven through a biochemically induced aggregation of the cytoskeleton. It is important to mention that a recent publication has shown that the incorporation of fluorescent probes into the membrane may extend the immiscibility regime in a three-component system [42]. This implies that macroscopic domain formation may be triggered in a pure POPC-SM-Cholesterol system at a temperature a few degrees lower than what is observed with the use of fluorescent probe labeling.

The macroscopic domains that appear during cooling in the giant vesicle system are irregular in shape. This indicates that these domains are unlikely to be formed by *lo*/*ld* phase coexistence. A recent report sustains that *lo*/*ld* phase coexistence is not observed in the POPC/SM/Cholesterol system, unless it is induced through light-damage [40]. In that work, only macroscopic domains involving *ld*/*so* phase coexistence are reported to form in the absence of light damage in systems involving a high melting lipid in combination with POPC and cholesterol. Our results agree with this previous report in that the platelet plasma membrane composition appears to lend itself only to the formation of *ld*/*so* macroscopic domains as the temperature is lowered. The question is then whether the fact that these domains may be formed by *ld*/*so* instead of *ld*/*lo* phase coexistence undermines the physiological usefulness of these large segregated regions in platelets. This is because the high rigidity and lack of lateral mobility provided by the *so* phase has led to a reputation for being “not physiologically useful”. However, it is clear that, at least for platelet activation, the reorganization of the platelet plasma membrane during cooling leads to activation of the platelets [23,25,44]. Accessing the *ld*/*so* phase coexistence during cooling will surely lead to a reorganization of membrane proteins and a change in local membrane protein concentrations which is likely to trigger activation. Therefore, even though the *so* phase may not serve to partition dynamically membrane proteins, its formation will definitely act as a trigger for membrane reorganization. Membrane phase behavior has been proposed previously as a physiological thermometer [45,46].

With regards to the recent working definition of rafts and the formation of larger platforms [17], the current results point to the possibility that larger platforms could be stabilized by lipid phase behavior. However, if lipid phase separation is truly happening in cells, it appears to require, at least in platelets, a low cholesterol content and a reduction in temperature. This may be grounds to exclude *so* phase formation as an accessible mechanism for triggering the appearance of platforms at physiological temperatures. However, the presence of high melting temperature lipids, such as ceramides may trigger the formation of *so* phase at physiological temperatures [36,47]. In addition, the irregular shaped domains observed in the model does not exclude the possible presence of *lo* phase, since these domains could emerge from *ld*/*lo*/*so* coexistence. The formation of *so* phase may assist in the aggregation of existing nanoscopic *lo* phase domains, providing an alternative mechanism to protein induced platform formation.

Although a recent publication shows that it is possible to generate GUVs from native erythrocyte membranes that maintain membrane asymmetry, we do not include in this work similar experiments with native platelet membranes. These experiments cannot be done properly due to experimental limitations. In contrast to erythrocytes, platelets are very sensitive to perturbations, and will activate in contact with surfaces such as the electrodes used during electroformation, and under any hydration stress induced during electroformation. Platelet activation results in a loss in lipid asymmetry. Therefore, it is very difficult to guarantee that platelet membrane asymmetry will be preserved during electroformation. Any results obtained for giant vesicles of native platelet membranes will be doubtful due to this technical limitation. The lack of a GUV system from native platelet membranes for direct comparison with the model system generates a gap in the argument of whether the thermotropic phase behavior of the platelets observed by FTIR does result in lipid induced macroscopic domain formation in platelets. However, the similarity in the temperature at which heterogeneous distribution of DiI emerges in platelets shown by Gousset et al. [25] and at which macroscopic domains

emerge in our model supports the validity of our model system. The thermal reversibility in the heterogeneity of DiI distribution in platelets observed by Gousset et al. indicates that this process is not mediated by biochemical signaling.

Acknowledgments

This work was supported by National Institute of Health grant HL61204, and by Basic Research Grant, COLCIENCIAS RC-156-2006.

References

1. Dietrich C, Bagatolli LA, Volovyk ZN, Thompson NL, Levi M, Jacobson K, Gratton E. Lipid rafts reconstituted in model membranes. Biophys J 2001;80:1417–1428. [PubMed: 11222302]
2. Mishra S, Joshi PG. Lipid raft heterogeneity: An enigma. J Neurochem 2007;103:135–142. [PubMed: 17986148]
3. Munro S. Lipid Rafts: Elusive or illusive? Cell 2003;115:377–388. [PubMed: 14622593]
4. Sengupta P, Holowka D, Baird B. Fluorescence resonance energy transfer between lipid probes detects nanoscopic heterogeneity in the plasma membrane of live cells. Biophys J 2007;92:3564–3574. [PubMed: 17325019]
5. Korlach J, Baumgart T, Webb WW, Feigenson GW. Detection of motional heterogeneities in lipid bilayer membranes by dual probe fluorescence correlation spectroscopy. Biochim Biophys Acta, Biomembr 2005;1668:158–163.
6. Bagatolli LA, Gratton E. Two photon fluorescence microscopy of coexisting lipid domains in giant unilamellar vesicles of binary phospholipid mixtures. Biophys J 2000;78:290–305. [PubMed: 10620293]
7. Veatch SL, Keller SL. Separation of liquid phases in giant vesicles of ternary mixtures of phospholipids and cholesterol. Biophys J 2003;85:3074–3083. [PubMed: 14581208]
8. Sharma P, Varma R, Sarasij RC, Ira, Gousset K, Krishnamoorthy G, Rao M, Mayor S. Nanoscale organization of multiple GPI-anchored proteins in living cell membranes. Cell 2004;116:577–589. [PubMed: 14980224]
9. Kusumi A, Suzuki K. Toward understanding the dynamics of membrane-raft-based molecular interactions. Biochim Biophys Acta, Mol Cell Res 2005;1746:234–251.
10. London E. How principles of domain formation in model membranes may explain ambiguities concerning lipid raft formation in cells. Biochim Biophys Acta, Mol Cell Res 2005;1746:203–220.
11. Yethiraj A, Weisshaar JC. Why are lipid rafts not observed in vivo? Biophys J 2007;93:3113–3119. [PubMed: 17660324]
12. Baumgart T, Hammond AT, Sengupta P, Hess ST, Holowka DA, Baird BA, Webb WW. Large-scale fluid/fluid phase separation of proteins and lipids in giant plasma membrane vesicles. Proc Natl Acad Sci U S A 2007;104:3165–3170. [PubMed: 17360623]
13. Gaus K, Gratton E, Kable EPW, Jones AS, Gelissen I, Kritharides L, Jessup W. Visualizing lipid structure and raft domains in living cells with two-photon microscopy. Proc Natl Acad Sci U S A 2003;100:15554–15559. [PubMed: 14673117]
14. Gómez-Moutón C, Abad JL, Mira E, Lacalle RA, Gallardo E, Jiménez-Baranda S, Illa I, Bernad A, Mañes S, Martínez-A C. Segregation of leading-edge and uropod components into specific lipid rafts during T cell polarization. Proc Natl Acad Sci U S A 2001;98:9642–9647. [PubMed: 11493690]
15. Qi SY, Groves JT, Chakraborty AK. Synaptic pattern formation during cellular recognition. Proc Natl Acad Sci U S A 2001;98:6548–6553. [PubMed: 11371622]
16. Mossman KD, Campi G, Groves JT, Dustin ML. Altered TCR signaling from geometrically repatterned immunological synapses. Science 2005;310:1191–1193. [PubMed: 16293763]
17. Pike LJ. Rafts defined: a report on the keystone symposium on lipid rafts and cell function. J Lipid Res 2006;47:1597–1598. [PubMed: 16645198]
18. Malínská K, Malínsky J, Opekarová M, Tanner W. Visualization of protein compartmentation within the plasma membrane of living yeast cells. Mol Biol Cell 2003;14:4427–4436. [PubMed: 14551254]

19. Schütz GJ, Kada G, Pastushenko VP, Schindler H. Properties of lipid microdomains in a muscle cell membrane visualized by single molecule microscopy. EMBO J 2000;19:892–901. [PubMed: 10698931]
20. Wang TY, Leventis R, Silvius JR. Artificially lipid-anchored proteins can elicit clustering-induced intracellular signaling events in Jurkat T-lymphocytes independent of lipid raft association. J Biol Chem 2005;280:22839–22846. [PubMed: 15817446]
21. Veatch SL, Keller SL. Miscibility Phase Diagrams of Giant Vesicles Containing Sphingomyelin. Phys Rev Lett 2005;94:148101. [PubMed: 15904115]
22. Tablin F, Wolkers WF, Walker NJ, Oliver AE, Tsvetkova NM, Gousset K, Crowe LM, Crowe JH. Membrane reorganization during chilling: Implications for long-term stabilization of platelets. Cryobiology 2001;43:114–123. [PubMed: 11846466]
23. Crowe JH, Tablin F, Tsvetkova N, Oliver AE, Walker N, Crowe LM. Are lipid phase transitions responsible for chilling damage in human platelets? Cryobiology 1999;38:180–191. [PubMed: 10328908]
24. Chernoff A, Snyder EL. The cellular and molecular basis of the platelet storage lesion: A symposium summary. Transfusion 1992;32:386–390. [PubMed: 1350121]
25. Gousset K, Wolkers WF, Tsvetkova NM, Oliver AE, Field CL, Walkers NJ, Crowe JH, Tablin F. Evidence for a physiological role for membrane rafts in human platelets. J Cell Phys 2002;190:117–128.
26. Tsvetkova NM, Crowe JH, Walker NJ, Crowe LM, Oliver AE, Wolkers WF, Tablin F. Physical properties of membrane fractions isolated from human platelets: implications for chilling induced platelet activation. Mol Mem Biol 1999;16:265–272.
27. Leidy C, Wolkers WF, Jorgensen K, Mouritsen OG, Crowe JH. Lateral organization and domain formation in a two-component lipid membrane system. Biophys J 2001;80:1819–1828. [PubMed: 11259295]
28. Arrondo JLR, Goñi FM. Infrared studies of protein-induced perturbation of lipids in lipoproteins and membranes. Chem Phys Lipids 1998;96:53–68. [PubMed: 9871982]
29. de Almeida RFM, Fedorov A, Prieto M. Sphingomyelin/phosphatidylcholine/cholesterol phase diagram: Boundaries and composition of lipid rafts. Biophys J 2003;85:2406–2416. [PubMed: 14507704]
30. Pokorny A, Yandek LE, Elegbede AI, Hinderliter A, Almeida PFF. Temperature and composition dependence of the interaction of {delta}-Lysin with ternary mixtures of sphingomyelin/cholesterol/POPC. Biophys J 2006;91:2184–2197. [PubMed: 16798807]
31. Tablin F, Oliver AE, Walker NJ, Crowe LM, Crowe JH. Membrane phase transition of intact human platelets: Correlation with cold-induced activation. J Cell Phys 1996;168:305–313.
32. Angelova M, Soléau S, Méléard P, Faucon F, Bothorel P. Preparation of giant vesicles by external AC electric fields. Kinetics and applications. Trends Colloid Interf Sci 1992;VI:127–131.
33. Mannock DA, Lewis RNAH, McElhaney RN. Comparative calorimetric and spectroscopic studies of the effects of lanosterol and cholesterol on the thermotropic phase behavior and organization of dipalmitoylphosphatidylcholine bilayer membranes. Biophys J 2006;91:3327–3340. [PubMed: 16905603]
34. McMullen TP, Lewis RN, McElhaney RN. Comparative differential scanning calorimetric and FTIR and 31P-NMR spectroscopic studies of the effects of cholesterol and androstenol on the thermotropic phase behavior and organization of phosphatidylcholine bilayers. Biophys J 1994;66:741–752. [PubMed: 8011906]
35. Chap HJ, Zwaal RFA, Van Deenen LLM. Action of highly purified phospholipases on blood platelets. Evidence for an asymmetric distribution of phospholipids in the surface membrane. Biochim Biophys Acta, Biomembr 1977;467:146–164.
36. Fidorra M, Duelund L, Leidy C, Simonsen AC, Bagatolli LA. Absence of fluid-ordered/fluid-disordered phase coexistence in ceramide/POPC mixtures containing cholesterol. Biophys J 2006;90:4437–4451. [PubMed: 16565051]
37. Blau L, Bittman R. Cholesterol distribution between the two halves of the lipid bilayer of human erythrocyte ghost membranes. J Biol Chem 1978;253:8366–8368. [PubMed: 711757]

38. Wang TY, Silvius JR. Cholesterol does not induce segregation of liquid-ordered domains in bilayers modeling the inner leaflet of the plasma membrane. Biophys J 2001;81:2762–2773. [PubMed: 11606289]

39. Leidy C, Wolkers WF, Oliver AE, Tsvetkova NM, Crowe LM, Tablin F, Crowe JH. Using FTIR to measure the partitioning of cholesterol in sphingomyelin/DPPC mixtures: Keys for the structural factors that determine the formation of cholesterol-enriched domains. Biophys J 2002;82:155A–255A.

40. Zhao J, Wu J, Shao H, Kong F, Jain N, Hunt G, Feigenson G. Phase studies of model biomembranes: Macroscopic coexistence of L[alpha] + L[beta], with light-induced coexistence of L[alpha] + Lo Phases. Biochim Biophys Acta, Biomembr 2007;1768:2777–2786.

41. Wolkers WF, Crowe LM, Tsvetkova NM, Tablin F, Crowe JH. In situ assessment of erythrocyte membrane properties during cold storage. Mol Mem Biol 2002;19:59–65.

42. Rodi PM, Trucco VM, Gennaro AM. Factors determining detergent resistance of erythrocyte membranes. Biophys Chem 2008;135:14–18. [PubMed: 18394774]

43. Veatch SL, Leung SSW, Hancock REW, Thewalt JL. Fluorescent Probes Alter Miscibility Phase Boundaries in Ternary Vesicles. J Phys Chem B 2007;111:502–504. [PubMed: 17228905]

44. Gousset K, Tsvetkova NM, Crowe JH, Tablin F. Important role of raft aggregation in the signaling events of cold-induced platelet activation. Biochim Biophys Acta, Biomembr 2004;1660:7–15.

45. Vígh, L.; Török, Z.; Balogh, G.; Glatz, A.; Piotto, S.; Horváth, I. Membrane-regulated stress response, Advances in experimental medicine and biology. In: Csermely, P.; Vígh, L., editors. Molecular Aspects of the Stress Response: Chaperones, Membranes and Networks. Vol. 594. Springer; N. Y.: 2007. p. 114-131.

46. Tsvetkova NM, Horváth I, Török Z, Wolkers WF, Balogi Z, Shigapova N, Crowe LM, Tablin F, Vierling E, Crowe JH, Vígh L. Small heat-shock proteins regulate membrane lipid polymorphism. Proc Natl Acad Sci U S A 2002;99:13504–13509. [PubMed: 12368478]

47. Castro BM, de Almeida RFM, Silva LC, Fedorov A, Prieto M. Formation of ceramide/sphingomyelin gel domains in the presence of an unsaturated phospholipid: A quantitative multiprobe approach. Biophys J 2007;93:1639–1650. [PubMed: 17496019]

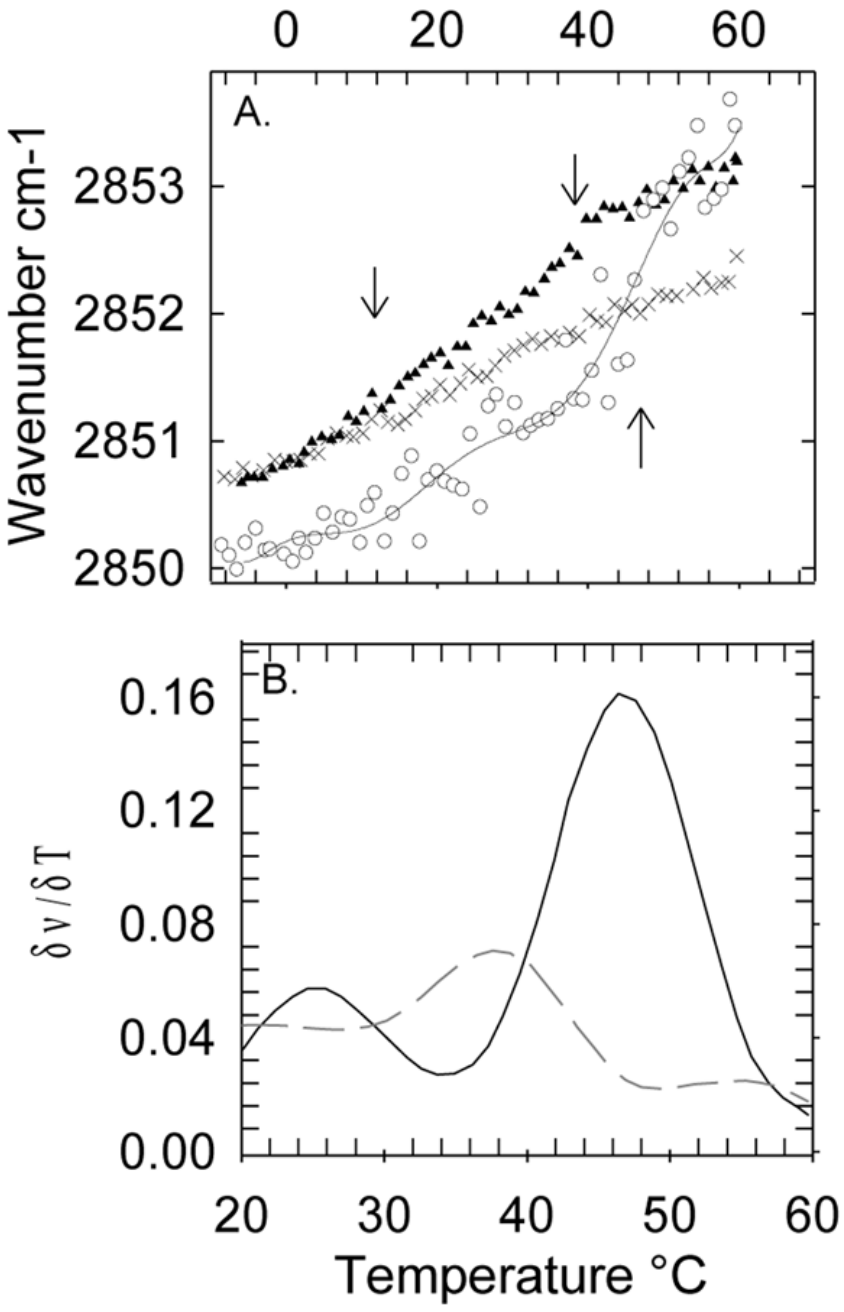

Figure 1.

(A) Thermotropic behavior of fresh platelets (x) as determined by monitoring the CH_2 symmetric stretch by FTIR. After treatment with β-CD (▲) platelets present two cooperative events at 15°C and 37°C indicated by the top arrows. The β-CD treated platelets are then exposed to SMase (○), and the cooperative event at 37°C shifts towards higher temperature, as shown by the bottom arrow, indicating the formation of ceramides. (B) For visual aid purposes, we plot the smoothed first derivative of the traces in (A) to show more clearly the cooperative event at 37°C (dashed line) after treatment with β-CD and its shift after treatment with SMase (solid line).

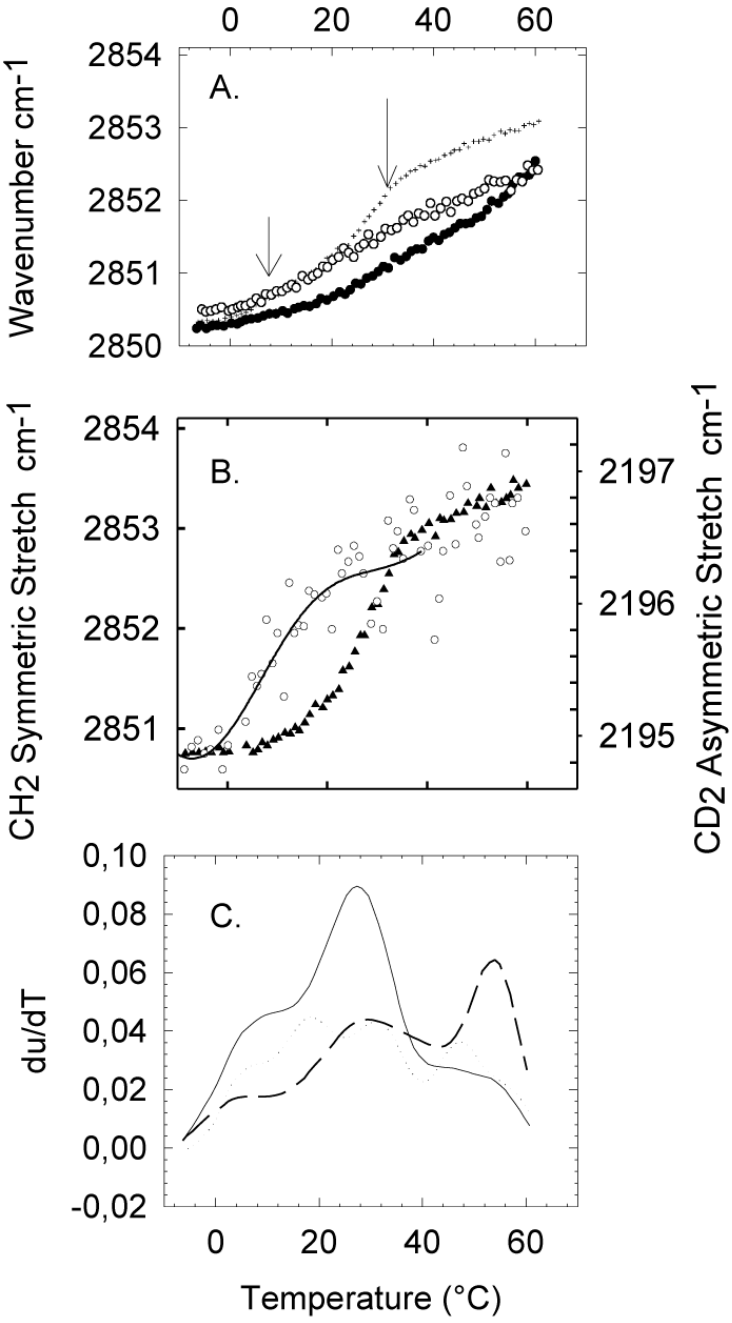

Figure 2.

Thermotropic phase behavior of a model membrane system representing the outer leaflet composition of the platelet plasma membrane as determined by monitoring the CH_2 symmetric stretch by FTIR. (A) A 55:30:15 POPC/SM/Cholesterol system (open circles) models the thermotropic phase behavior of the platelet plasma membrane before treatment with β-CD. A 55:30 POPC/SM system (black crosses) represents the thermotropic phase behavior of platelets after treatment with β-CD. The 55:30 POPC/SM system was treated with SMase (black circles), which after treatment shows two cooperative events at 27°C and 50°C. Arrows point to the two cooperative melting events before SMase treatment. (B) The cooperative phase behavior of the 55:30 POPC/SM system is studied in more detail by monitoring the CD_2 stretch of POPC-

d31 and the CH_2 stretch of SM, showing that a POPC rich population melts at 10°C and a SM rich population melts at 27°C. C) For visual aid purposes, we plot the smoothed first derivative of the traces in (A) for the 55:30:15 POPC/SM/Cholesterol system (dotted line), 55:30 POPC/SM system (solid line), and 55:30 POPC/SM system treated with SMase (dashed line).

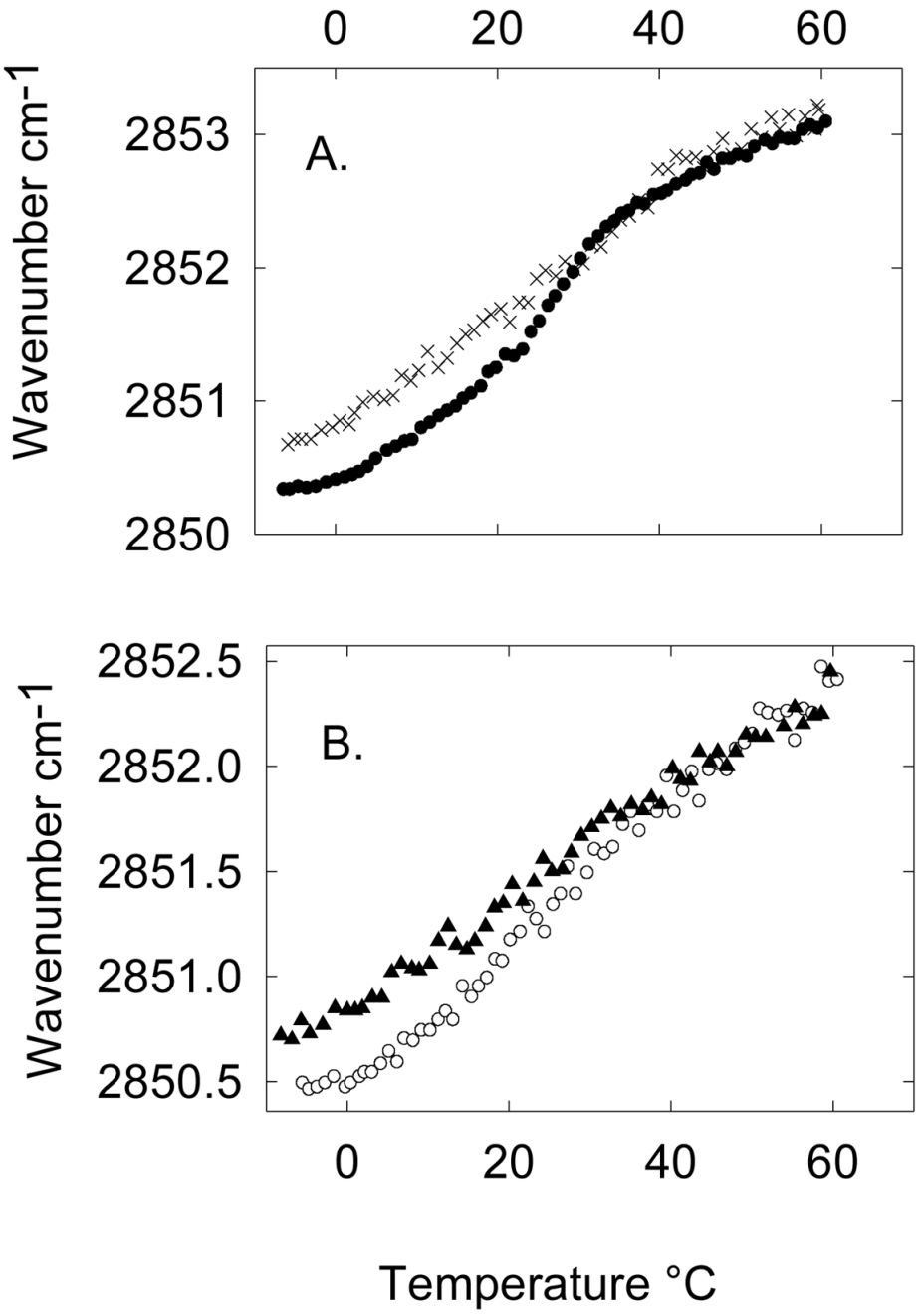

Figure 3.

Comparison between the thermotropic phase behavior of the platelet system and the 55:30 POPC/SM model system representing the outer leaflet composition of the platelet plasma membrane in the (A) **a**bsence (× represent the platelets after treatment with β-CD and ● represent the 55:30 POPC/SM model system) and (B) presence of cholesterol (▲ represent fresh ○ platelets and represent the 55:30:15 POPC/SM/Cholesterol model system) as determined by monitoring the CH_2 symmetric stretch by FTIR.

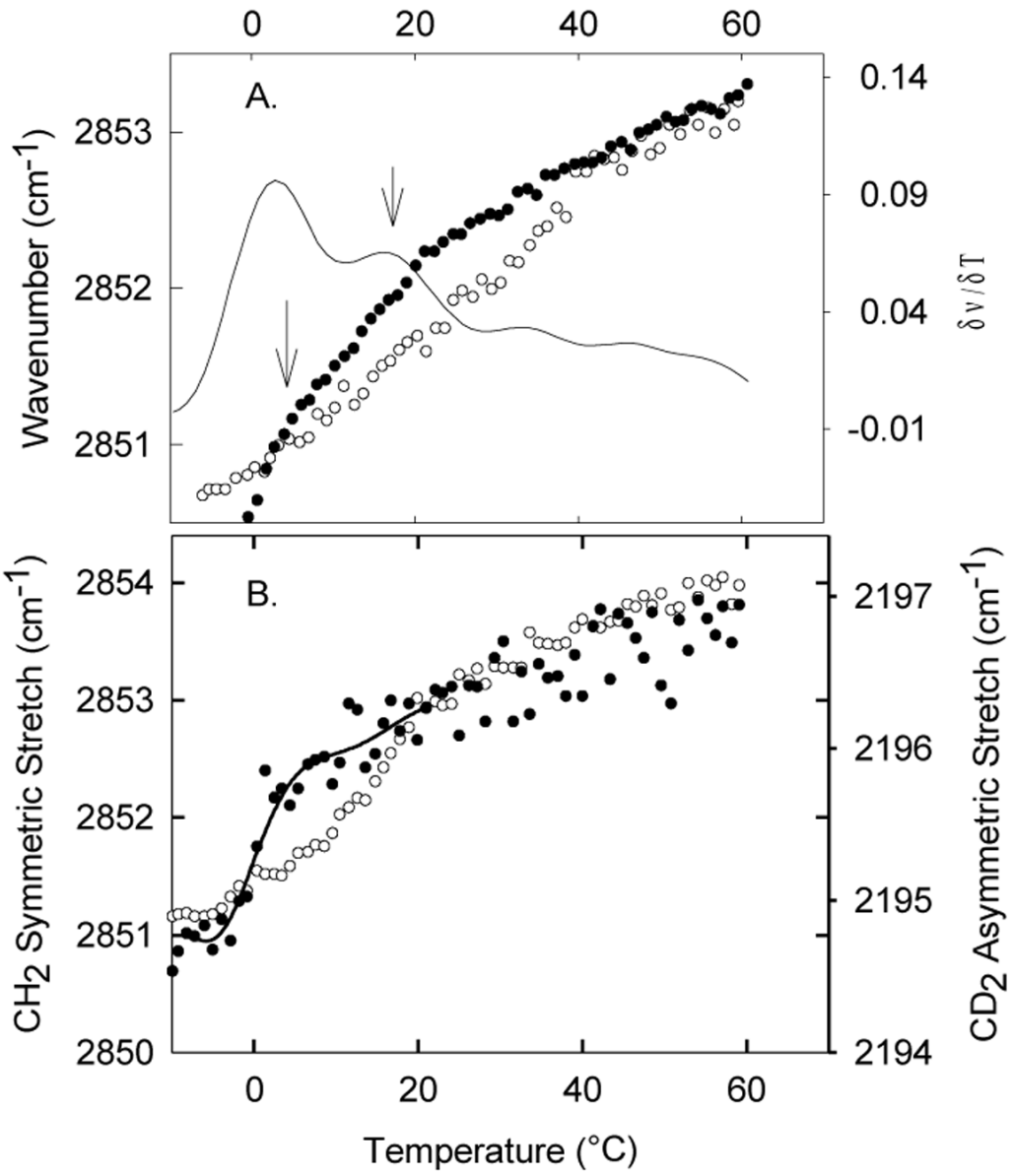

Figure 4.

Thermotropic phase behavior of a model membrane system representing the platelet plasma membrane composition that does not assume an asymmetric lipid distribution as determined by monitoring the CH_2 symmetric stretch by FTIR. (A) A 70:15 POPC/SM system before (closed circles, ●) and after (open circles,○) SMase treatment. The solid line trace shows the smoothed first derivative of the 70:15 POPC/SM system before treatment with SMase, which is used as a visual aid to point out the cooperative events. (B) The cooperative phase behavior of the 70:15 POPC/SM system is studied in more detail by monitoring the CD_2 stretch of POPC d-31 (black circles,●) and the CH_2 stretch of SM (open circles,○), showing that a POPC rich population melts at 2°C and a SM rich population melts just below 20°C.

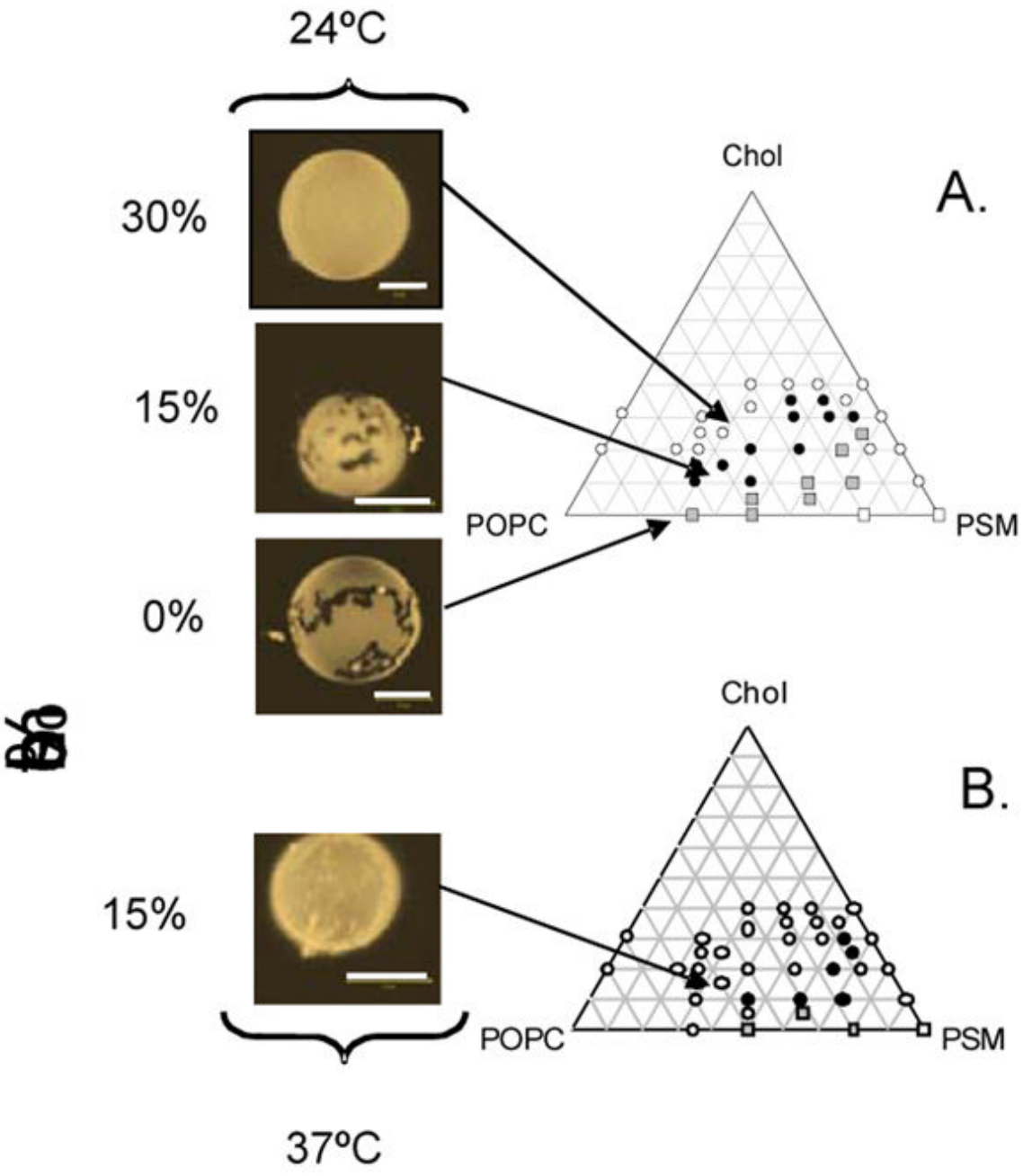

Figure 5.

Giant unilamellar vesicles were grown from a 55:30 POPC/BSM stock containing 0, 15 and 30 mol % cholesterol and imaged at 24°C (Upper Panel). All vesicles were labeled with 0.5 mol% DiIC18:0. The 15 mol% cholesterol sample, which represents the composition of the outer leaflet of the platelet plasma membrane, presents macroscopic domain formation. The giant vesicle are compared with a recently published POPC/PSM/Chol phase diagram (7) showing that at 15 mol% the sample enters the region for macroscopic domains at 24°C (closed circles in phase diagram). Lower Panel shows a 55:30 POPC/BSM sample containing 15 mol % cholesterol at 37°C. No macroscopic domains are observed at this temperature. Comparison

with the POPC/PSM/Chol phase diagram (7) shows that, for this composition and temperature, the system is located in a one phase region (open circles in phase diagram)

Table 1

Composition and lipid distribution of the platelet plasma membrane leads to a model tertiary mixture that mimics the outer leaflet. Two different models are considered assuming symmetric or asymmetric lipid distribution

Headgroups	% wt resting platelets Tsvetkova et al. 1999	Inner leaflet/outer leaflet distribution	3 Component model for the outer leaflet assuming asymmetric distribution(in wt ratio)	3 Component model for the outer leaflet assuming asymmetric distribution(in mol%)	Outer leaflet model assuming symmetric distribution of SM where PC accounts for all other phospholipids (in mol %)
FFA	5.2±0.6	not determined			
PE	25.3±0.4	(+++) inner leaflet			
PS	6.4±0.4	(+++) inner leaflet			
PG	–	–			
PI	5.8±0.3	(+++) inner leaflet			
PC	34.8±0.1	(+) outer leaflet	55	55	70
SM	14.6±0.2	(+++) outer leaflet	30	30	15
Cholesterol	7.5±0.6	even	7.5	15	15

(FFA) free fatty acids, (PE) phosphatidylethalonamine, (PS) phosphatidyl serine, (PG) phosphatidylglycerol, (PI) phosphatidylinositol, (PC) phosphatidylcholine, (SM) sphingomyelin.